

TINA: Text-Free Inversion Attack for Unlearned Text-to-Image Diffusion Models

Qianlong Xiang^{1,2,3}, Miao Zhang^{1,†}, Haoyu Zhang^{1,4}, Kun Wang⁵, Junhui Hou², Liqiang Nie^{1,3,†}
¹Harbin Institute of Technology (Shenzhen) ²City University of Hong Kong ³Shenzhen Loop Area Institute
⁴Peng Cheng Laboratory ⁵Shandong University
<https://github.com/qianlong0502/TINA>

Abstract

Although text-to-image diffusion models exhibit remarkable generative power, concept erasure techniques are essential for their safe deployment to prevent the creation of harmful content. This has fostered a dynamic interplay between the development of erasure defenses and the adversarial probes designed to bypass them, and this co-evolution has progressively enhanced the efficacy of erasure methods. However, this adversarial co-evolution has converged on a narrow, text-centric paradigm that equates erasure with severing the text-to-image mapping, ignoring that the underlying visual knowledge related to undesired concepts still persist. To substantiate this claim, we investigate from a visual perspective, leveraging DDIM inversion to probe whether a generative pathway for the erased concept can still be found. However, identifying such a visual generative pathway is challenging because standard text-guided DDIM inversion is actively resisted by text-centric defenses within the erased model. To address this, we introduce TINA, a novel Text-free INversion Attack, which enforces this visual-only probe by operating under a null-text condition, thereby avoiding existing text-centric defenses. Moreover, TINA integrates an optimization procedure to overcome the accumulating approximation errors that arise when standard inversion operates without its usual textual guidance. Our experiments demonstrate that TINA regenerates erased concepts from models treated with state-of-the-art unlearning. The success of TINA proves that current methods merely obscure concepts, highlighting an urgent need for paradigms that operate directly on internal visual knowledge.

1. Introduction

With the rapid development of deep learning [16–18, 40–45, 53–55], generative artificial intelligence, particularly Text-to-Image (T2I) diffusion models such as Stable Diffusion is fundamentally reshaping the landscape of digital

[†]Corresponding authors

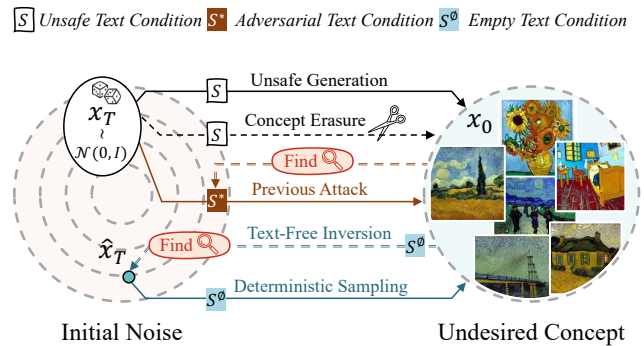


Figure 1. Conceptual overview of text-centric erasure vulnerabilities and our TINA attack. **Concept Erasure** usually severs the link between a specific text condition and the undesired concept. **Previous Attacks** remain text-centric, finding adversarial text condition to reactivate the concept. **Our TINA** bypasses the text pathway entirely. Using an empty text condition, it finds a noise to regenerate the concept, proving the visual knowledge persists in the existing erased models.

content creation [24, 28, 30, 32, 49]. Their remarkable capacity for creative synthesis has catalyzed countless applications, from art and design to entertainment and media. However, since these models are typically trained on massive, unfiltered datasets scraped from the Internet [35], their proliferation brings a turbulent undercurrent of ethical and safety challenges. The same models that generate breathtaking art can be misused to create deepfakes that violate personal privacy [2], imitate artistic styles that infringe on copyright [13, 31, 36], and produce harmful Not-Safe-For-Work (NSFW) imagery [12, 34, 57], posing significant risks to intellectual property and societal well-being.

To address these challenges, the field has converged on the paradigm of *Concept Erasure*, a specialized form of *Machine Unlearning* [50]. This paradigm aims to mitigate risks by directly modifying model parameters. For instance, approaches such as Erasing Stable Diffusion (ESD) and Ablating Concepts (AC) retrain specific model layers to remap a forbidden concept representation to that of a neutral or null

concept, thereby severing the explicit link between a text prompt and its corresponding visual output [6, 15]. Other methods like Forget-Me-Not (FMN) minimize the attention maps corresponding to the target concept [52], while Unified Concept Editing (UCE) applies efficient, closed-form edits to the cross-attention weights [7]. Despite their distinct mechanisms, these approaches share a common, text-centric operational principle, equating erasure with merely severing its *text-image mapping*.

The text-centric paradigm, as conceptualized in Figure 1, has consequently guided adversarial attacks almost exclusively to the textual domain. Initial red-teaming efforts involve prompt-level manipulations, attempting to find alternative phrasings or complex prompts that reactivate the target concept [4, 39, 57]. Moreover, the more sophisticated embedding-space attacks, which move beyond discrete tokens, remain fundamentally dependent on the textual conditioning pathway [27]. Generally, these red-teaming methods aim to discover new token embeddings [27] or optimize an adversarial text prompt [57] that serves as a proxy for the erased concept. In response to this threat, an interplay between text-based attacks and defenses has driven the subsequent development of more resilient safeguards, such as AdvUnlearn [56] and STEREO [38]. This adversarial co-evolution has produced defenses that demonstrate increasing efficacy, thereby fostering an appearance of robust model security.

However, in this work, we contend that this competitive co-evolution of text-centric methods rests on a fundamental and fatal assumption. Specifically, existing paradigm mistakenly equates the erasure of a *text-to-image link* with the far more complex task of eliminating the underlying *visual knowledge* from the parameter space. Consequently, existing methods critically ignore the fact that even if textual inputs can no longer induce the target concept, the corresponding visual knowledge may still persist, untapped, within the model. To challenge this dominant paradigm and substantiate our claim, we introduce a core hypothesis:

A deterministic generative pathway for an erased concept persists within the model, even after its text-image mappings are removed, allowing for its regeneration in a completely text-free manner.

To validate this hypothesis from a purely visual perspective, thereby challenging the efficacy of these text-centric defenses, we introduce TINA, a Text-free INversion Attack. Unlike prior embedding-space attacks that seek a new textual proxy for the erased concept [27], TINA is a novel framework designed to completely bypass the textual conditioning pathway. To achieve this, TINA leverages Denoising Diffusion Implicit Models (DDIM) [37] inversion as a visual probe (illustrated in Figure 1), allowing us to investigate the visual knowledge embedded within the model directly. However, identifying such a generative pathway is

challenging because standard DDIM inversion relies heavily on textual guidance. Operating under the null-text condition necessary to evade defenses consequently introduces significant imprecision. To address this imprecision, TINA incorporates a novel optimization procedure that corrects for the compounding errors of standard inversion, allowing it to precisely map a target image back to a latent noise vector. Serving as the specific initial noise for the deterministic DDIM sampling process, this resulting latent vector can lead an erased model to regenerate the forbidden content through a deterministic generative trajectory, entirely bypassing the text-conditioning mechanism. The success of this text-free reconstruction provides compelling evidence that current erasure methods merely obscure concepts by severing text-image links, rather than truly expunging the underlying visual knowledge embedded deep within the model parameters. These findings serve as a critical alert for the AI safety community, highlighting the urgent need for more robust unlearning paradigms that operate directly on the internal visual representations within T2I models.

To sum up, our contributions are as follows.

- To our knowledge, we are the first to identify the fundamental, text-centric vulnerability in the current paradigm of concept erasure for T2I diffusion models.
- We propose TINA, a new text-free attack paradigm that employs an optimization-based inversion to identify the underlying generative trajectory for a supposedly erased concept, from a purely visual perspective.
- Experiments demonstrate that our TINA can rediscover erased concepts from models unlearned by state-of-the-art methods, thereby exposing a fundamental flaw needing urgent attention.

2. Related Work

2.1. Text-to-Image Diffusion Models

The advent of Text-to-Image (T2I) diffusion models, such as Stable Diffusion [30], DALL-E 2 [29], and Imagen [32], has marked a paradigm shift in digital content generation. These models operate through a two-stage process: a forward diffusion process that incrementally adds noise to an image, and a learned reverse process that denoises a random vector back into a coherent image [11]. To achieve computational efficiency, models like Stable Diffusion perform this process in a lower-dimensional latent space [30]. Critically, their generative process is guided by textual prompts, typically encoded and injected into the denoising network via a cross-attention mechanism [40]. This tight coupling between text and image synthesis is the source of their remarkable controllability, but also the root of significant safety and ethical concerns, as the models can be prompted to produce NSFW imagery [34, 57], imitate copyrighted styles [13, 36], or violate personal privacy [2].

2.2. Concept Erasure in Diffusion Models

To address the misuse of T2I models, concept erasure has emerged as a critical field. While methods like SLD [34] focus on inference-time interventions, the dominant paradigm involves fine-tuning-based methods that modify model parameters. This paradigm originated with foundational works like ESD [6] and AC [15], which retrained models to break associations with specific text prompts. Subsequently, this was followed by more efficient and targeted techniques, such as FMN [52], UCE [7], MACE [20], and the adapter-based SPM [21], often focusing on cross-attention layers. Concurrently, general unlearning frameworks like SalUn [5], Scissorhands [47], and EraseDiff [48] were proposed for the concept erasure task. As text-based attacks began to bypass these initial erasure methods, advanced adversarially robust methods were developed, including RECE [8], AdvUnlearn [56], and STEREO [38]. These methods usually integrate attack considerations into their design to defend against adversarial prompts and embeddings. Ultimately, this co-evolution of text-based attacks and defenses has solidified a dominant, text-centric paradigm: most of them operate by identifying or severing the *text-to-image mapping*, rather than addressing the underlying visual knowledge.

2.3. Adversarial Attacks on Concept Erasure

The prevailing text-centric assumption of erasure methods has consequently shaped the landscape of adversarial attacks, which primarily seek to circumvent these textual defenses. These attacks can be classified by their operational domain. The most straightforward approaches operate in the discrete token space, employing circumvention strategies to find alternative phrases that trigger the erased concept, such as P4D [4], RAB [39], MMA [51], and UDA [57]. A more sophisticated class of attacks operates in the continuous embedding space. These methods aim to find a novel token embedding that acts as a proxy for the forbidden concept, effectively creating a new activation pathway to the visual knowledge. For instance, CCE [27] leverages textual inversion to discover surrogate embeddings for erased concepts.

Critically, despite their varying levels of sophistication, from simple phrasings to optimized vectors, these existing attacks share a fundamental limitation: most of them presuppose that the generative capabilities of the model must be accessed via its text-conditioning pathway. They focus on finding a new textual or embedding-space vector to bypass modified controls. In stark contrast, our work, TINA, challenges this entire paradigm. We pivot to a fundamentally different attack surface by postulating that visual knowledge persists independently of any textual control. Accordingly, we propose an attack that circumvents the text-conditioning mechanism entirely, identifying and

exploiting a deterministic, non-textual generative trajectory to regenerate forbidden content without textual guidance.

3. Method

3.1. Preliminaries

Latent Diffusion Models. Latent Diffusion Models (LDMs) [30] generate images by reversing a T -step diffusion process in a compressed latent space. An image x is first encoded into its latent $z_0 = \mathcal{E}(x)$ by a VAE encoder. The forward process creates a sequence of noised latents $\{z_1, \dots, z_T\}$. A denoising U-Net ϵ_θ learns to reverse this process. At each timestep t , it predicts the noise ϵ in z_t , guided by a textual condition c . This condition is produced by a text encoder $\mathcal{T}_{\text{text}}$ from a prompt y and integrated via cross-attention. The training objective minimizes the noise prediction error:

$$\mathcal{L} = \mathbb{E}_{z_0, y, \epsilon, t} \left[\|\epsilon - \epsilon_\theta(z_t, t, c)\|_2^2 \right].$$

This objective trains ϵ_θ to denoise z_t back towards z_0 in a manner faithful to the condition c . The final image is retrieved using the VAE decoder \mathcal{D} .

DDIM Sampling. Denoising Diffusion Implicit Models (DDIM) [37] enable deterministic generative sampling from LDMs. This is achieved by formulating the reverse process as a non-Markovian, discretized Probability Flow Ordinary Differential Equation (PF-ODE) with zero variance. Consequently, for a fixed model θ and condition c , any initial noise $z_T \sim \mathcal{N}(0, \mathbf{I})$ maps to a unique generated latent z_0 .

This deterministic path is defined by an iterative update rule. Given the latent z_t , the model first predicts the clean latent $\hat{z}_0(z_t)$:

$$\hat{z}_0(z_t) = \frac{z_t - \sqrt{1 - \alpha_t} \epsilon_\theta(z_t, t, c)}{\sqrt{\alpha_t}}. \quad (1)$$

The preceding latent z_{t-1} is then computed as:

$$z_{t-1} = \sqrt{\alpha_{t-1}} \hat{z}_0(z_t) + \sqrt{1 - \alpha_{t-1}} \cdot \epsilon_\theta(z_t, t, c), \quad (2)$$

where $\{\alpha_t\}_{t=1}^T$ are the fixed noise schedule parameters.

DDIM Inversion. Building upon the deterministic nature of DDIM sampling, DDIM inversion provides a mechanism to reverse the generative process. Its objective is to map a given image, represented by its initial latent z_0 , back to the unique starting noise vector z_T from which it can be deterministically generated. This capability is crucial for applications like real image editing and analysis.

Ideally, the inversion would be a perfect algebraic reversal of the sampling step in Eq. (2), which can be expressed as:

$$z_t = C_1(t)z_{t-1} + C_2(t) \cdot \epsilon_\theta(z_t, t, c), \quad (3)$$

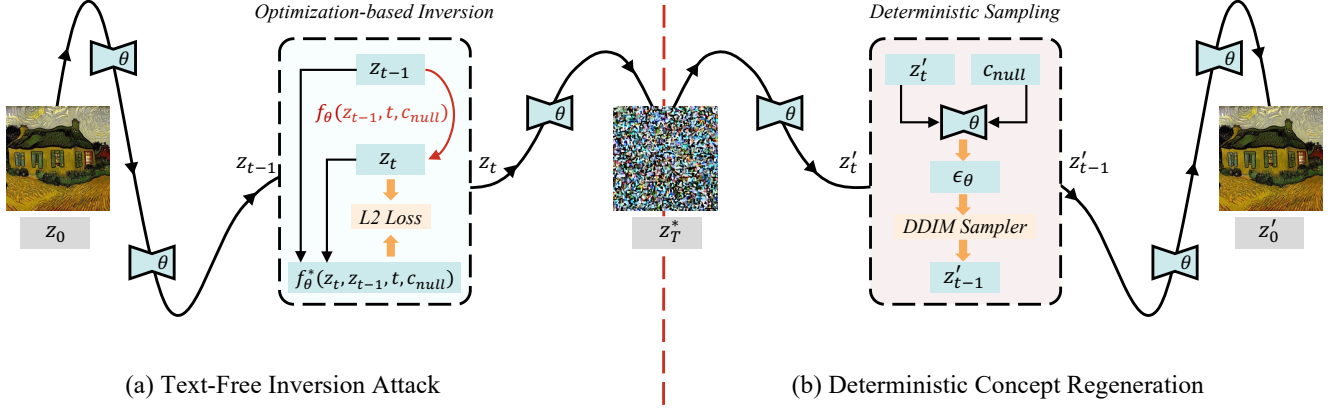


Figure 2. The TINA (Text-free INversion Attack) framework. (a) **Text-Free Inversion Attack**: An optimization-based, null-text (c_{null}) inversion finds the unique initial noise z_T^* corresponding to a target image z_0 . This optimization corrects the errors from standard inversion. (b) **Deterministic Concept Regeneration**: The *same* sanitized model θ uses z_T^* and c_{null} to deterministically regenerate the target concept z'_0 , proving the visual knowledge persists despite erasure.

where

$$C_1(t) = \frac{\sqrt{\alpha_t}}{\sqrt{\alpha_{t-1}}}, \quad (4)$$

$$C_2(t) = \sqrt{1 - \alpha_t} - \sqrt{\frac{\alpha_t(1 - \alpha_{t-1})}{\alpha_{t-1}}}. \quad (5)$$

However, a practical challenge emerges: computing the latent z_t requires a noise prediction $\epsilon_\theta(z_t, t, c)$, which itself depends on z_t , as shown in Eq. (3). To break this circular dependency, standard DDIM inversion employs a key approximation: it estimates the required noise using the latent from the previous step, z_{t-1} , at timestep $t - 1$. This results in the following iterative formula to approximate z_t from z_{t-1} :

$$z_t \approx f_\theta(z_{t-1}, t, c), \quad (6)$$

where

$$f_\theta(z_{t-1}, t, c) = C_1(t)z_{t-1} + C_2(t) \cdot \epsilon_\theta(z_{t-1}, t - 1, c). \quad (7)$$

Starting from the clean image latent z_0 , this equation is applied sequentially for $t = 1, \dots, T$ to trace the trajectory back to an approximate initial noise \hat{z}_T . This vector serves as an estimate of the true starting point in the noise space required for reconstructing the original image.

3.2. TINA: Text-free INversion Attack

In this section, we introduce our TINA framework, starting with the attack pipeline (Section 3.2.1), then analyzing why the naive standard inversion fails to meet the objective in the pipeline (Section 3.2.2), and finally detailing our optimization-based solution (Section 3.2.3).

3.2.1. The TINA Attack Pipeline

The central hypothesis of TINA is that even within a model subjected to concept erasure, deterministic generative trajectories persist that are entirely independent of textual conditioning. Our framework is designed to expose and exploit this vulnerability through a two-phase attack pipeline, as illustrated in Figure 2.

The process begins with a concept-erased model ϵ_θ and a target image x representing the erased concept. As illustrated in Figure 2, the attack first performs a **Text-Free Inversion** to find the precise initial noise vector z_T^* that corresponds to the target image latent z_0 . This inversion phase uses only the sanitized model ϵ_θ and a null-text condition c_{null} . Following this, in the **Deterministic Regeneration** phase, this optimized z_T^* is fed back into the *same* erased model ϵ_θ . A standard deterministic DDIM sampling process is then executed, crucially starting from this specific z_T^* and operating entirely under the null-text condition c_{null} .

The successful reconstruction of the target concept x' serves as definitive proof that the visual knowledge persists, independent of textual controls. The deterministic regeneration step is a standard DDIM sampling procedure; the core technical challenge lies in the initial inversion step: accurately identifying the starting noise vector z_T^* for a target image x representing the erased concept.

3.2.2. Limitations of Standard Inversion

A naive approach to finding z_T^* would be to apply the standard DDIM inversion process to the target image latent z_0 . However, this method is fundamentally flawed and fails in two distinct ways, as illustrated in Figure 3. First, if the inversion is attempted using the text condition c of the target concept (e.g., ‘‘Van Gogh style’’), the sanitized model ϵ_θ actively counteracts this prompt, leading to a complete failure

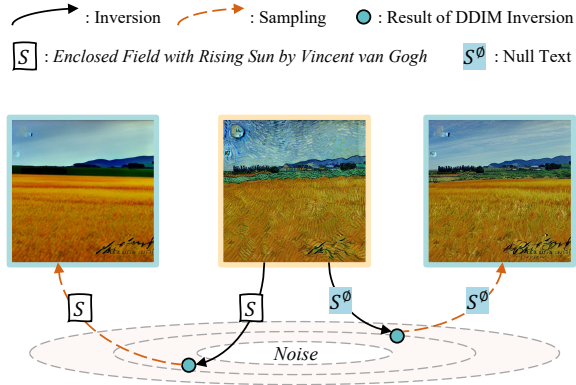


Figure 3. Standard DDIM inversion fails to find the generative trajectory. The text-guided path (S) is blocked by the erasure, while the null-text path (S^\emptyset) drifts due to approximation errors, failing to restore the target concept.

in reconstruction. This confirms that text-centric defenses are indeed working against text-guided processes.

Second, we could attempt the inversion under a null-text condition ($c = c_{\text{null}}$) to bypass this textual defense. This approach also fails, but in a more subtle way. As shown in Figure 3 (right), the resulting image is visually closer to the original than the text-conditioned attempt, yet it still fails to regenerate the specific target concept (i.e., the artistic style). This partial failure stems from the standard inversion formula (Eq. (6)), which relies on a critical approximation: it uses the noise prediction from the previous step, $\epsilon_\theta(z_{t-1}, t-1, c)$, to estimate the next latent z_t . This approximation is heavily dependent on a meaningful text condition c to guide the noise prediction. In the absence of such guidance (c_{null}), the predictions become unconstrained, and the small error introduced at each step rapidly compounds across the entire trajectory. Consequently, the final computed noise \hat{z}_T drifts sufficiently from the true required noise z_T^* to lose the high-fidelity details of the target concept, rendering it incapable of an accurate reconstruction. This demonstrates that standard inversion is an inadequate tool for identifying text-free generative paths.

3.2.3. Optimization-Based Text-Free Inversion

To overcome the imprecision of approximative inversion, TINA reframes the search for the generative trajectory as an optimization problem. We discard the flawed approximation in Eq. (6) and instead derive the ideal inversion relationship directly from the DDIM sampling equation (Eq. (2)). By algebraically rearranging the sampling step, we can express the exact, non-approximative relationship between z_t and z_{t-1} :

$$z_t = C_1(t)z_{t-1} + C_2(t) \cdot \epsilon_\theta(z_t, t, c). \quad (8)$$

Algorithm 1 TINA: Text-Free Inversion

- 1: **Input:** Sanitized denoising model ϵ_θ , target image latent z_0 , DDIM steps T , null-text condition c_{null} , max optimization iterations K , learning rate η .
 - 2: **Output:** Optimized initial noise z_T^* .
 - 3: **for** $t \leftarrow 1$ to T **do**
 - 4: Get initial \tilde{z}_t from z_{t-1} using Eq. (6) with c_{null} .
 - 5: $z_t \leftarrow \tilde{z}_t$.
 - 6: **for** $k \leftarrow 1$ to K **do**
 - 7: $\mathcal{L}_t \leftarrow \|f_\theta^*(z_t, z_{t-1}, t, c_{\text{null}}) - z_t\|_2^2 \triangleright$ Eq. (10)
 - 8: $z_t \leftarrow z_t - \eta \nabla_{z_t} \mathcal{L}_t$
 - 9: **end for**
 - 10: **end for**
 - 11: $z_T^* \leftarrow z_T$
 - 12: **return** z_T^*
-

This equation establishes an implicit consistency constraint that must hold at every step of a true generative trajectory. We can therefore cast the exact inversion at step t as a **fixed-point problem**. In particular, for fixed z_{t-1} , t , and c , any exact latent z_t on the DDIM trajectory must satisfy a self-consistency relation of the form $z_t = f_\theta^*(z_t, z_{t-1}, t, c)$, i.e., z_t is a fixed point of the induced mapping f_θ^* [1, 25]. Let us define f_θ^* as:

$$f_\theta^*(z_t, z_{t-1}, t, c) = C_1(t)z_{t-1} + C_2(t) \cdot \epsilon_\theta(z_t, t, c). \quad (9)$$

Our key innovation is to enforce this self-consistency constraint at each step of the inversion process through optimization, rather than relying on the approximative closed-form update. For each timestep t from 1 to T , given the previously computed z_{t-1} , we seek a latent z_t whose induced denoising prediction is consistent with the exact DDIM relation under a null-text condition. We formulate this as the following loss function:

$$\mathcal{L}_t(z_t) = \|f_\theta^*(z_t, z_{t-1}, t, c_{\text{null}}) - z_t\|_2^2, \quad (10)$$

where z_t is initialized as $\tilde{z}_t = f_\theta(z_{t-1}, t, c_{\text{null}})$ before the optimization.

Instead of accepting the erroneous result from the standard formula, we employ an inner optimization loop at each inversion step t . We first obtain an initial estimate for z_t using the conventional DDIM inversion step (Eq. (6)) under the null-text condition. This estimate then serves as the starting point for an iterative refinement process where we perform gradient descent on z_t to minimize the objective defined in Eq. (10). In this sense, our optimization can be viewed as seeking a numerically self-consistent point, rather than directly trusting the approximative inversion formula [25]. This optimization forces each latent z_t along the inversion path to be consistent with the internal dynamics of the sanitized model ϵ_θ in a text-free setting. The inner loop is exe-

cuted for a fixed number of iterations. By iteratively applying this optimization-based refinement for $t = 1, \dots, T$, we trace a highly accurate path back to the true initial noise z_T^* , which is now completely decoupled from any textual influence. The complete procedure for this text-free inversion is formally detailed in Algorithm 1.

4. Experiments

4.1. Experimental Setup

Unlearned DMs to be attacked. The field of machine unlearning for diffusion models is advancing at a rapid pace. For our evaluation, we select target unlearning methods based on two criteria: the public availability of their source code and the reproducibility of their reported results. Specifically, our evaluation targets twelve prominent, open-source unlearning methods: (1) ESD (erased stable diffusion) [6], (2) FMN (Forget-Me-Not) [52], (3) AC (ablating concepts) [15], (4) UCE (unified concept editing) [7], (5) EraseDiff [48], (6) Scissorhands [47], (7) MACE (Mass Concept Erasure) [20], (8) SPM (concept-SemiPermeable Membrane) [21], (9) RECE [8], (10) AdvUnlearn [56], (11) SalUn (saliency unlearning) [5], (12) STEREO [38]. We note that these unlearning methods are often specialized for specific domains (e.g., nudity) rather than being universal. Consequently, our evaluation is contextualized, assessing each method only on its intended unlearning tasks.

Baseline Attack Methods. We evaluate the attack performance of TINA against five prevailing baseline attack methods: (1) MMA [51], (2) Prompting4Debugging (P4D) [4], (3) UnlearnDiffAtk (UDA) [57], (4) Ring-A-Bell (RAB) [39], and (5) CCE [27]. The fundamental characteristic and shared limitation of all these baselines is their text-centric nature. They exclusively target the textual input pathway in an attempt to circumvent textual defenses. These approaches range from black-box jailbreaking techniques that discover alternative text prompts (e.g., MMA, RAB) to white-box attacks that leverage model access to optimize for adversarial text conditions (e.g., P4D, UDA, CCE). Critically, all these existing attacks remain tethered to the text-conditioning mechanism, a pathway that TINA is designed to bypass entirely. As summarized in Table 3, not all baseline attacks are designed for every type of concept (e.g., MMA and RAB are not applicable to style or object erasure). Therefore, our comparative analysis is conducted on a per-task basis, aligning with the intended application of each attack method. The implementing details of these baselines can be found in Appendix 6.

Image Setup. Our method requires a set of representative images, each exemplifying a concept targeted for erasure. We obtain these images by adopting the generation

setup established in the UnlearnDiffAtk (UDA) study [57]. This process involves using the original Stable Diffusion v1.4 model, which is the pre-trained checkpoint before any unlearning methods were applied, to generate a collection of ground-truth images. The generation is guided by text prompts sourced from the same standard benchmarks used to evaluate the baseline attacks. Specifically, for nudity concepts, we use prompts from the I2P dataset [34]. For artistic styles, we focus our experiments on the Van Gogh style, using art-related prompts from the ESD evaluation setup [6]. For objects, we concentrate on the tench class, using prompts generated via GPT-4 corresponding to this Imagenette class, following the methodology in [57].

Implementation Details. All experiments are built upon the Stable Diffusion v1.4 checkpoint. For all generative processes, we employ a linear multistep scheduler with $T = 50$ inference steps and a standard Classifier-Free Guidance (CFG [10]) scale of 7.5. For our proposed TINA, the optimization-based inversion (detailed in Section 3.2 and Algorithm 1) is also configured with $T = 50$ total steps. Within the inner optimization loop at each timestep t , we perform $K = 25$ refinement iterations to minimize the fixed-point loss (Eq. 10). This inner optimization uses the AdamW [19] with a learning rate of $\eta = 0.001$. All experiments were conducted on a single NVIDIA A100 GPU.

Evaluation Metrics. Our evaluation methodology is primarily aligned with the protocol established by UnlearnDiffAtk (UDA) [57]. To quantitatively measure attack efficacy, we report the Attack Success Rate (ASR), defined as the percentage of generated images that are successfully identified by a post-generation classifier as containing the forbidden concept, thereby indicating a successful bypass of the unlearning safeguard. We employ a suite of specialized classifiers corresponding to each unlearning task. For harmful concept unlearning, we utilize NudeNet to detect nudity. For style unlearning, we adopt the 129-class ViT-base style classifier [46, 57], which was pre-trained on ImageNet, fine-tuned on the WikiArt dataset [33]. For object unlearning, we employ a standard ImageNet-pretrained ResNet-50 [9] for generated image classification.

4.2. Experiment Results

We now empirically validate the efficacy of TINA. Our experiments are designed to test the ability of TINA to bypass a wide spectrum of unlearning defenses, from foundational methods to the current state-of-the-art, and compare its performance directly against existing text-centric attacks. The results for nudity, style, and object erasure are summarized in Tables 1, 2, and 4, respectively. Qualitative comparisons and an ablation study are provided in Figure 4, Section 11, and Appendix 7.

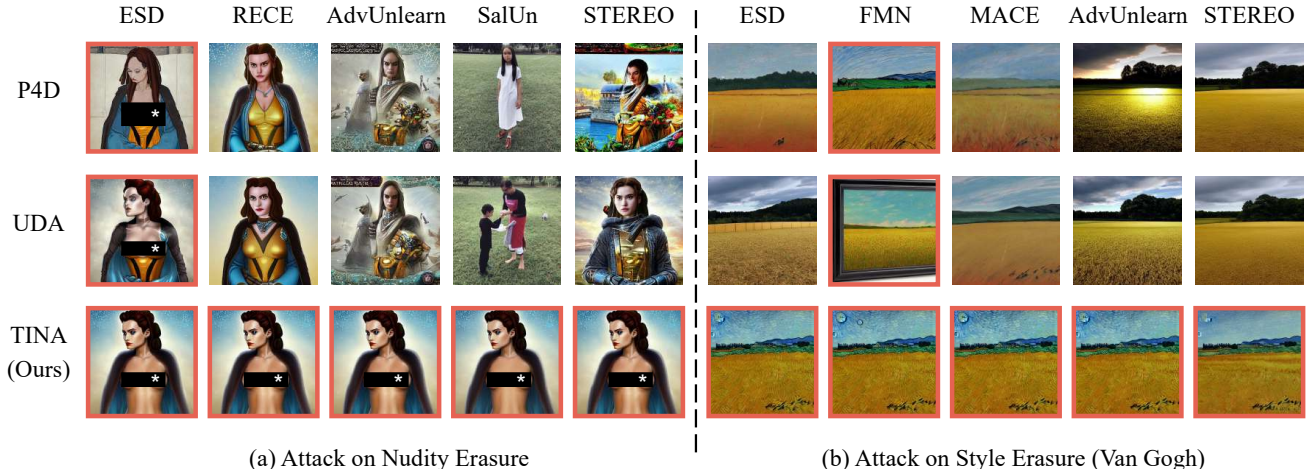


Figure 4. Qualitative comparison of attack performance on (a) Nudity Erasure and (b) Style Erasure (Van Gogh). Images with a **red border** indicate a successful attack. Our TINA (bottom row) consistently regenerates the forbidden concepts, bypassing most of defenses, while text-centric attacks fail against robust methods. Sensitive content is redacted.

	ESD [6]	FMN [52]	UCE [7]	MACE [20]	RECE [8]	AdvUnlearn [56]	SalUn [5]	STEREO [38]
MMA [51]	13.10	67.00	32.60	6.00	22.80	1.70	1.70	5.50
P4D [4]	69.01	97.89	76.06	75.35	66.20	18.31	15.49	24.65
UDA [57]	76.05	97.89	78.87	81.69	63.38	23.24	13.38	25.35
RAB [39]	50.53	97.89	29.47	6.32	10.53	2.11	0.00	8.42
CCE [27]	74.65	54.93	49.30	50.00	66.90	76.76	2.82	16.90
TINA	82.39	97.89	82.39	92.96	80.28	78.87	71.13	80.99

Table 1. Quantitative comparison of Attack Success Rates (ASR, in %) on the nudity erasure task. We evaluate our TINA against five baselines across eight prominent unlearning defenses. **Bold** indicates the best-performing attack.

Evaluation on Erased Models in Nudity Erasure. Table 1 demonstrates comprehensive success of TINA in the nudity erasure task. TINA achieves the highest ASR across all eight defenses. It reaches 82.39% against ESD and 92.96% against MACE, significantly outperforming all baselines. The most critical finding is the performance of TINA against defenses designed to be robust, such as AdvUnlearn, SalUn, and STEREO. Against these targets, text-based attacks are largely mitigated (e.g., UDA scores 23.24% on AdvUnlearn, RAB scores 0.00% on SalUn). In contrast, TINA maintains high ASRs (78.87%, 71.13%, and 80.99%), proving it exploits a vulnerability that these defenses do not account for. This quantitative success is visually corroborated in Figure 4 (a). The bottom row shows TINA consistently regenerating the target content across all defenses. In contrast, text-centric attacks like P4D and UDA visibly fail against robust methods such as AdvUnlearn and STEREO, producing neutral or unrelated images.

Evaluation on Erased Models in Style Erasure. The results for artistic style erasure (Table 2) further reinforce this

trend. TINA robustly bypasses the majority of defenses. Its 70.0% ASR against ESD starkly contrasts with the 32.0% from UDA and 8.0% from CCE. Furthermore, TINA shows dominant performance against robust methods like AdvUnlearn (70.0%) and STEREO (44.0%), where text-based attacks remain weak or ineffective. This finding demonstrates that even for abstract concepts like style, a deterministic, non-textual generative trajectory persists after erasure, which TINA successfully identifies and exploits. Figure 4 (b) provides the qualitative evidence for this trend. It clearly demonstrates the ability of TINA to restore the “Van Gogh” style, bypassing defenses like MACE and AdvUnlearn where text-based attacks fail to regenerate the artistic features.

Evaluation on Erased Models in Object Erasure. The object erasure evaluation in Table 4 delivers the most compelling results. This task highlights the failure of text-centric unlearning against our text-free attack. Against modern defenses like Scissorhands and STEREO, all text-based attacks (P4D, UDA, and CCE) fail catastrophically,

	ESD [6]	FMN [52]	AC [15]	MACE [20]	SPM [21]	RECE [8]	AdvUnlearn [56]	STEREO [38]
P4D [4]	30.0	54.0	68.0	42.0	78.0	62.0	0.0	0.0
UDA [57]	<u>32.0</u>	<u>56.0</u>	77.0	<u>56.0</u>	88.0	<u>64.0</u>	2.0	0.0
CCE [27]	8.0	18.0	14.0	26.0	36.0	40.0	<u>44.0</u>	<u>4.0</u>
TINA	70.0	72.0	<u>74.0</u>	72.0	<u>80.0</u>	74.0	70.0	44.0

Table 2. Comparison of Attack Success Rates (ASR, in %) on the artistic style erasure task. We report the performance of our TINA against three baselines across eight unlearning methods. **Bold** denotes the highest ASR, while underlined denotes the second highest.

	MMA	P4D	UDA	RAB	CCE
Nudity	✓	✓	✓	✓	✓
Style	✗	✓	✓	✗	✓
Object	✗	✓	✓	✗	✓

Table 3. Applicability of baseline attack methods to different tasks. ✓ denotes applicability, while ✗ denotes non-applicability.

	P4D	UDA	CCE	TINA
ESD [6]	32.0	46.0	40.0	70.0
EraseDiff [48]	8.0	2.0	34.0	68.0
SalUn [5]	18.0	12.0	58.0	72.0
Scissorhands [47]	6.0	6.0	0.0	78.0
STEREO [38]	0.0	2.0	2.0	72.0

Table 4. Attack Success Rates (ASR, in %) for object erasure. Our TINA bypasses modern defenses where text-centric attacks fail.

with ASRs in the single digits. While P4D and UDA also fail against EraseDiff and SalUn, the embedding-space attack CCE retains partial efficacy (34.0% and 58.0%, respectively). This pattern confirms that while robust defenses are patching textual vulnerabilities, TINA remains unaffected. It achieves uniformly high ASRs across all targets, including 68.0% (EraseDiff), 78.0% (Scissorhands), and 72.0% (STEREO). This finding confirms our central hypothesis: current SOTA methods merely sever text-image links, not the underlying visual knowledge, which TINA can deterministically access without any textual guidance.

4.3. Latent Embedding Analysis

To further understand the generative pathway identified by TINA, we visualize the learned noise embeddings z_T^* for four erased concepts (Tench, Church, Parachute, Garbage Truck) using a t-SNE projection. Specifically, for each concept, we collect 50 optimized noise vectors generated by targeting the corresponding ESD-sanitized model. We then feed these optimized noises into the UNet under a null-text condition and extract their intermediate representations through a forward inference. For the visualization, we apply t-SNE (perplexity 30, with PCA initialization)

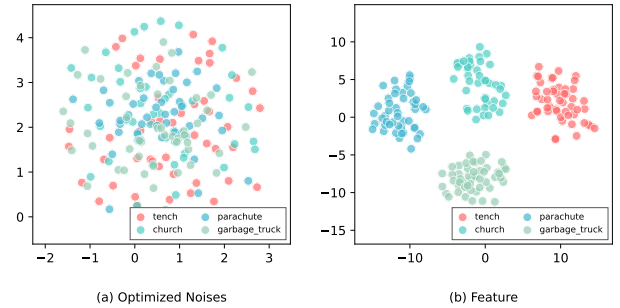


Figure 5. t-SNE visualization of (a) the optimized initial noises z_T^* and (b) their corresponding deep UNet activations (extracted from the `mid_block`) for four erased concepts.

to both the flattened noise vectors and the global average pooled features extracted from the last ResNet block of the `mid_block` in the UNet model. As shown in Figure 5, the optimized noises themselves (left) exhibit little concept-wise separation in the latent space, which is consistent with their noise-like nature. However, their corresponding internal UNet activations (right) become clearly separable by concept, forming distinct clusters. This demonstrates that although the optimized z_T^* remains indistinguishable from random noise, it successfully elicits concept-specific internal responses within the erased diffusion model. This confirms that the forbidden visual knowledge persists and is deterministically activated by our text-free attack.

5. Conclusion

We exposed a fundamental flaw in the text-centric paradigm of concept erasure: severing text-image links is insufficient and offers a false sense of security. We introduced TINA, a novel text-free attack that substantiates this claim by completely bypassing textual controls. TINA identifies a deterministic, null-text generative trajectory to regenerate forbidden content. Our experiments show that TINA consistently restores erased concepts from models sanitized by existing defenses. This proves current methods merely obscure visual knowledge rather than erasing it, mandating a shift towards unlearning techniques that operate directly on internal visual representations.

References

- [1] Stefan Banach. Sur les opérations dans les ensembles abstraits et leur application aux équations intégrales. *Fundamenta mathematicae*, 3(1):133–181, 1922. 5
- [2] Nicolas Carlini, Jamie Hayes, Milad Nasr, Matthew Jagielski, Vikash Sehwal, Florian Tramèr, Borja Balle, Daphne Ippolito, and Eric Wallace. Extracting training data from diffusion models. In *32nd USENIX security symposium (USENIX Security 23)*, pages 5253–5270, 2023. 1, 2
- [3] Junsong Chen, Jincheng YU, Chongjian GE, Lewei Yao, Enze Xie, Zhongdao Wang, James Kwok, Ping Luo, Huchuan Lu, and Zhenguo Li. Pixart- α : Fast training of diffusion transformer for photorealistic text-to-image synthesis. In *The Twelfth International Conference on Learning Representations*, 2024. 14
- [4] Zhi-Yi Chin, Chieh-Ming Jiang, Ching-Chun Huang, Pin-Yu Chen, and Wei-Chen Chiu. Prompting4debugging: Red-teaming text-to-image diffusion models by finding problematic prompts. *arXiv preprint arXiv:2309.06135*, 2023. 2, 3, 6, 7, 8, 12
- [5] Chongyu Fan, Jiancheng Liu, Yihua Zhang, Eric Wong, Dennis Wei, and Sijia Liu. Salun: Empowering machine unlearning via gradient-based weight saliency in both image classification and generation. *arXiv preprint arXiv:2310.12508*, 2023. 3, 6, 7, 8, 13
- [6] Rohit Gandikota, Joanna Materzynska, Jaden Fiotto-Kaufman, and David Bau. Erasing concepts from diffusion models. In *Proceedings of the IEEE/CVF international conference on computer vision*, pages 2426–2436, 2023. 2, 3, 6, 7, 8, 13, 14
- [7] Rohit Gandikota, Hadas Orgad, Yonatan Belinkov, Joanna Materzynska, and David Bau. Unified concept editing in diffusion models. In *Proceedings of the IEEE/CVF Winter Conference on Applications of Computer Vision*, pages 5111–5120, 2024. 2, 3, 6, 7
- [8] Chao Gong, Kai Chen, Zhipeng Wei, Jingjing Chen, and Yungang Jiang. Reliable and efficient concept erasure of text-to-image diffusion models. In *European Conference on Computer Vision*, pages 73–88. Springer, 2024. 3, 6, 7, 8
- [9] Kaiming He, Xiangyu Zhang, Shaoqing Ren, and Jian Sun. Deep residual learning for image recognition. In *Proceedings of the IEEE conference on computer vision and pattern recognition*, pages 770–778, 2016. 6
- [10] Jonathan Ho and Tim Salimans. Classifier-free diffusion guidance. *arXiv preprint arXiv:2207.12598*, 2022. 6
- [11] Jonathan Ho, Ajay Jain, and Pieter Abbeel. Denoising diffusion probabilistic models. *Advances in neural information processing systems*, 33:6840–6851, 2020. 2
- [12] Tatum Hunter. Ai porn is easy to make now. for women, that’s a nightmare. *The Washington Post*, pages NA–NA, 2023. 1
- [13] Harry H Jiang, Lauren Brown, Jessica Cheng, Mehtab Khan, Abhishek Gupta, Deja Workman, Alex Hanna, Johnathan Flowers, and Timnit Gebru. Ai art and its impact on artists. In *Proceedings of the 2023 AAAI/ACM Conference on AI, Ethics, and Society*, pages 363–374, 2023. 1, 2
- [14] Xuan Ju, Ailing Zeng, Yuxuan Bian, Shaoteng Liu, and Qiang Xu. Pnp inversion: Boosting diffusion-based editing with 3 lines of code. In *The Twelfth International Conference on Learning Representations*, 2023. 13
- [15] Nupur Kumari, Bingliang Zhang, Sheng-Yu Wang, Eli Shechtman, Richard Zhang, and Jun-Yan Zhu. Ablating concepts in text-to-image diffusion models. In *Proceedings of the IEEE/CVF International Conference on Computer Vision*, pages 22691–22702, 2023. 2, 3, 6, 8
- [16] Zaijing Li, Yuquan Xie, Rui Shao, Gongwei Chen, Weili Guan, Dongmei Jiang, Yaowei Wang, and Liqiang Nie. Optimus-3: Dual-router aligned mixture-of-experts agent with dual-granularity reasoning-aware policy optimization. *arXiv preprint arXiv:2506.10357*, 2025. 1
- [17] Zaijing Li, Bing Hu, Rui Shao, Gongwei Chen, Dongmei Jiang, Pengwei Xie, Jianye Hao, and Liqiang Nie. Global prior meets local consistency: Dual-memory augmented vision-language-action model for efficient robotic manipulation. *arXiv preprint arXiv:2602.20200*, 2026.
- [18] Fan Liu, Yaqi Liu, Huilin Chen, Zhiyong Cheng, Liqiang Nie, and Mohan Kankanhalli. Understanding before recommendation: Semantic aspect-aware review exploitation via large language models. *ACM Transactions on Information Systems*, 43(2):1–26, 2025. 1
- [19] Ilya Loshchilov and Frank Hutter. Decoupled weight decay regularization. *arXiv preprint arXiv:1711.05101*, 2017. 6
- [20] Shilin Lu, Zilan Wang, Leyang Li, Yanzhu Liu, and Adams Wai-Kin Kong. Mace: Mass concept erasure in diffusion models. In *Proceedings of the IEEE/CVF Conference on Computer Vision and Pattern Recognition*, pages 6430–6440, 2024. 3, 6, 7, 8
- [21] Mengyao Lyu, Yuhong Yang, Haiwen Hong, Hui Chen, Xuan Jin, Yuan He, Hui Xue, Jungong Han, and Guiguang Ding. One-dimensional adapter to rule them all: Concepts diffusion models and erasing applications. In *Proceedings of the IEEE/CVF Conference on Computer Vision and Pattern Recognition*, pages 7559–7568, 2024. 3, 6, 8
- [22] Daiki Miyake, Akihiro Iohara, Yu Saito, and Toshiyuki Tanaka. Negative-prompt inversion: Fast image inversion for editing with text-guided diffusion models. In *2025 IEEE/CVF Winter Conference on Applications of Computer Vision (WACV)*, pages 2063–2072. IEEE, 2025. 13
- [23] Ron Mokady, Amir Hertz, Kfir Aberman, Yael Pritch, and Daniel Cohen-Or. Null-text inversion for editing real images using guided diffusion models. In *Proceedings of the IEEE/CVF conference on computer vision and pattern recognition*, pages 6038–6047, 2023. 13
- [24] Alex Nichol, Prafulla Dhariwal, Aditya Ramesh, Pranav Shyam, Pamela Mishkin, Bob McGrew, Ilya Sutskever, and Mark Chen. Glide: Towards photorealistic image generation and editing with text-guided diffusion models. *arXiv preprint arXiv:2112.10741*, 2021. 1
- [25] James M Ortega and Werner C Rheinboldt. *Iterative solution of nonlinear equations in several variables*. SIAM, 2000. 5
- [26] William Peebles and Saining Xie. Scalable diffusion models with transformers. In *Proceedings of the IEEE/CVF international conference on computer vision*, pages 4195–4205, 2023. 14

- [27] Minh Pham, Kelly O Marshall, Niv Cohen, Govind Mittal, and Chinmay Hegde. Circumventing concept erasure methods for text-to-image generative models. *arXiv preprint arXiv:2308.01508*, 2023. 2, 3, 6, 7, 8, 12
- [28] Aditya Ramesh, Mikhail Pavlov, Gabriel Goh, Scott Gray, Chelsea Voss, Alec Radford, Mark Chen, and Ilya Sutskever. Zero-shot text-to-image generation. In *International conference on machine learning*, pages 8821–8831. Pmlr, 2021. 1
- [29] Aditya Ramesh, Prafulla Dhariwal, Alex Nichol, Casey Chu, and Mark Chen. Hierarchical text-conditional image generation with clip latents. *arXiv preprint arXiv:2204.06125*, 1(2):3, 2022. 2
- [30] Robin Rombach, Andreas Blattmann, Dominik Lorenz, Patrick Esser, and Björn Ommer. High-resolution image synthesis with latent diffusion models. In *Proceedings of the IEEE/CVF conference on computer vision and pattern recognition*, pages 10684–10695, 2022. 1, 2, 3
- [31] Kevin Roose. An ai-generated picture won an art prize. artists aren’t happy. *New York Times*, 16(01):2025, 2022. 1
- [32] Chitwan Saharia, William Chan, Saurabh Saxena, Lala Li, Jay Whang, Emily L Denton, Kamyar Ghasemipour, Raphael Gontijo Lopes, Burcu Karagol Ayan, Tim Salimans, et al. Photorealistic text-to-image diffusion models with deep language understanding. *Advances in neural information processing systems*, 35:36479–36494, 2022. 1, 2
- [33] Babak Saleh and Ahmed Elgammal. Large-scale classification of fine-art paintings: Learning the right metric on the right feature. *arXiv preprint arXiv:1505.00855*, 2015. 6
- [34] Patrick Schramowski, Manuel Brack, Björn Deiseroth, and Kristian Kersting. Safe latent diffusion: Mitigating inappropriate degeneration in diffusion models. In *Proceedings of the IEEE/CVF Conference on Computer Vision and Pattern Recognition*, pages 22522–22531, 2023. 1, 2, 3, 6, 12
- [35] Christoph Schuhmann, Romain Beaumont, Richard Vencu, Cade Gordon, Ross Wightman, Mehdi Cherti, Theo Coombes, Aarush Katta, Clayton Mullis, Mitchell Wortsman, et al. Laion-5b: An open large-scale dataset for training next generation image-text models. *Advances in neural information processing systems*, 35:25278–25294, 2022. 1
- [36] Gowthami Somepalli, Vasu Singla, Micah Goldblum, Jonas Geiping, and Tom Goldstein. Diffusion art or digital forgery? investigating data replication in diffusion models. In *Proceedings of the IEEE/CVF conference on computer vision and pattern recognition*, pages 6048–6058, 2023. 1, 2
- [37] Jiaming Song, Chenlin Meng, and Stefano Ermon. Denoising diffusion implicit models. *arXiv preprint arXiv:2010.02502*, 2020. 2, 3, 13
- [38] Koushik Srivatsan, Fahad Shamshad, Muzammal Naseer, Vishal M Patel, and Karthik Nandakumar. Stereo: A two-stage framework for adversarially robust concept erasing from text-to-image diffusion models. In *Proceedings of the Computer Vision and Pattern Recognition Conference*, pages 23765–23774, 2025. 2, 3, 6, 7, 8, 13, 14
- [39] Yu-Lin Tsai, Chia-Yi Hsu, Chulin Xie, Chih-Hsun Lin, Jia-You Chen, Bo Li, Pin-Yu Chen, Chia-Mu Yu, and Chun-Ying Huang. Ring-a-bell! how reliable are concept removal methods for diffusion models? *arXiv preprint arXiv:2310.10012*, 2023. 2, 3, 6, 7, 12
- [40] Ashish Vaswani, Noam Shazeer, Niki Parmar, Jakob Uszkoreit, Llion Jones, Aidan N Gomez, Lukasz Kaiser, and Illia Polosukhin. Attention is all you need. *Advances in neural information processing systems*, 30, 2017. 1, 2
- [41] Kun Wang, Hao Liu, Lirong Jie, Zixu Li, Yupeng Hu, and Liqiang Nie. Explicit granularity and implicit scale correspondence learning for point-supervised video moment localization. In *Proceedings of the 32nd ACM International Conference on Multimedia*, pages 9214–9223, 2024.
- [42] Kun Wang, Yupeng Hu, Hao Liu, Lirong Jie, and Liqiang Nie. Redundancy mitigation: Towards accurate and efficient image-text retrieval. *IEEE Transactions on Circuits and Systems for Video Technology*, 2025.
- [43] Kun Wang, Yupeng Hu, Hao Liu, Jiang Shao, and Liqiang Nie. Cross-modal representation shift refinement for point-supervised video moment retrieval. *ACM Transactions on Information Systems*, 44(3):1–30, 2026.
- [44] Xiaolei Wang, Tianhong Dai, Huihui Bai, Yao Zhao, and Jimin Xiao. Unifying reconstruction and density estimation via invertible contraction mapping in one-class classification. In *The Thirty-ninth Annual Conference on Neural Information Processing Systems*, 2025.
- [45] Xiaolei Wang, Xiaoyang Wang, Huihui Bai, Eng Gee Lim, and Jimin Xiao. Decad: Decoupling anomalies in latent space for multi-class unsupervised anomaly detection. In *Proceedings of the IEEE/CVF International Conference on Computer Vision*, pages 21568–21577, 2025. 1
- [46] Bichen Wu, Chenfeng Xu, Xiaoliang Dai, Alvin Wan, Peizhao Zhang, Zhicheng Yan, Masayoshi Tomizuka, Joseph Gonzalez, Kurt Keutzer, and Peter Vajda. Visual transformers: Token-based image representation and processing for computer vision. *arXiv preprint arXiv:2006.03677*, 2020. 6
- [47] Jing Wu and Mehrtaash Harandi. Scissorhands: Scrub data influence via connection sensitivity in networks. In *European Conference on Computer Vision*, pages 367–384. Springer, 2024. 3, 6, 8, 13
- [48] Jing Wu, Trung Le, Munawar Hayat, and Mehrtaash Harandi. Erasediff: Erasing data influence in diffusion models. *arXiv preprint arXiv:2401.05779*, 2024. 3, 6, 8, 13
- [49] Qianlong Xiang, Miao Zhang, Yuzhang Shang, Jianlong Wu, Yan Yan, and Liqiang Nie. Dkdm: Data-free knowledge distillation for diffusion models with any architecture. In *Proceedings of the IEEE/CVF Conference on Computer Vision and Pattern Recognition*, pages 2955–2965, 2025. 1
- [50] Heng Xu, Tianqing Zhu, Lefeng Zhang, Wanlei Zhou, and Philip S. Yu. Machine unlearning: A survey. *ACM Comput. Surv.*, 56(1), 2023. 1
- [51] Yijun Yang, Ruiyuan Gao, Xiaosen Wang, Tsung-Yi Ho, Nan Xu, and Qiang Xu. Mma-diffusion: Multimodal attack on diffusion models. In *Proceedings of the IEEE/CVF Conference on Computer Vision and Pattern Recognition*, pages 7737–7746, 2024. 3, 6, 7, 12
- [52] Gong Zhang, Kai Wang, Xingqian Xu, Zhangyang Wang, and Humphrey Shi. Forget-me-not: Learning to forget in text-to-image diffusion models. In *Proceedings of*

- the IEEE/CVF conference on computer vision and pattern recognition*, pages 1755–1764, 2024. [2](#), [3](#), [6](#), [7](#), [8](#)
- [53] Haoyu Zhang, Meng Liu, Yuhong Li, Ming Yan, Zan Gao, Xiaojun Chang, and Liqiang Nie. Attribute-guided collaborative learning for partial person re-identification. *IEEE Transactions on Pattern Analysis and Machine Intelligence*, 45(12):14144–14160, 2023. [1](#)
- [54] Haoyu Zhang, Meng Liu, Zixin Liu, Xuemeng Song, Yaowei Wang, and Liqiang Nie. Multi-factor adaptive vision selection for egocentric video question answering. In *Forty-first International Conference on Machine Learning*, pages 59310–59328, 2024.
- [55] Haoyu Zhang, Meng Liu, Zaijing Li, Haokun Wen, Weili Guan, Yaowei Wang, and Liqiang Nie. Spatial understanding from videos: Structured prompts meet simulation data. In *Advances in Neural Information Processing Systems*, pages 1–16, 2025. [1](#)
- [56] Yimeng Zhang, Xin Chen, Jinghan Jia, Yihua Zhang, Chongyu Fan, Jiancheng Liu, Mingyi Hong, Ke Ding, and Sijia Liu. Defensive unlearning with adversarial training for robust concept erasure in diffusion models. *Advances in neural information processing systems*, 37:36748–36776, 2024. [2](#), [3](#), [6](#), [7](#), [8](#)
- [57] Yimeng Zhang, Jinghan Jia, Xin Chen, Aochuan Chen, Yihua Zhang, Jiancheng Liu, Ke Ding, and Sijia Liu. To generate or not? safety-driven unlearned diffusion models are still easy to generate unsafe images... for now. In *European Conference on Computer Vision*, pages 385–403. Springer, 2024. [1](#), [2](#), [3](#), [6](#), [7](#), [8](#), [12](#)
- [58] Ziyue Zhang, Mingbao Lin, Shuicheng YAN, and Rongrong Ji. Easyinv: Toward fast and better ddim inversion. In *Forty-second International Conference on Machine Learning*, 2025. [13](#)

TINA: Text-Free Inversion Attack for Unlearned Text-to-Image Diffusion Models

Supplementary Material

6. Baseline Attack Setup

We evaluate the robustness of the proposed method against five existing attack methods: MMA [51], Prompting4Debugging (P4D) [4], UnlearnDiffAtk (UDA) [57], Ring-A-Bell (RAB) [39] and CCE [27]. The details are presented below.

- **MMA** [51]: This method provides a publicly available set of 1,000 adversarial prompts, curated to bypass safeguards and generate nudity content, specifically targeting Stable Diffusion v1.5. Given that these prompts are designed for NSFW generation, we employ this dataset as a black-box attack to evaluate robustness on the nudity erasure task. For each unlearned diffusion model, our protocol involves using these 1,000 prompts as text conditions to generate 1,000 corresponding images. A fixed random seed is used for each generation to ensure reproducibility. The resulting images are subsequently evaluated using NudeNet to detect nudity and calculate the Attack Success Rate (ASR).
- **UDA** (UnlearnDiffAtk) [57]: This white-box attack aims to find a prompt that minimizes the denoising error of the sanitized model with respect to images containing the forbidden concepts. To ensure a fair comparison, we strictly follow the original attack setup. For the nudity task, we use 142 prompts from the I2P dataset [34] and set the number of optimized tokens to $N = 5$. For the artistic style (Van Gogh) and object (tench) tasks, we use 50 prompts each, with $N = 3$ optimized tokens. In all tasks, the adversarial perturbations are optimized for 40 iterations over 50 diffusion timesteps, using the AdamW optimizer with a 0.01 learning rate, consistent with the methodology in [57].
- **P4D** (Prompting4Debugging) [4]: This white-box attack requires access to both the original vanilla model and the target sanitized model. Its objective is to optimize an adversarial prompt c' that forces the sanitized model's noise prediction to match the original prediction of the model under the forbidden prompt c . To ensure a fair comparison, our P4D implementation strictly follows the experimental setup of UDA, using the identical prompt sets, the same number of optimized tokens ($N = 5$ for nudity, $N = 3$ for style/object), and the same optimization parameters (40 iterations, AdamW optimizer, 0.01 learning rate).
- **RAB** (Ring-A-Bell) [39]: This attack method is specifically designed to generate adversarial prompts for bypassing nudity safeguards. Therefore, we evaluate this attack exclusively on the nudity erasure task. We employ

the 95 adversarial prompts released by the official RAB implementation. As detailed in the original paper [39], this set of 95 prompts is generated by modifying the base I2P nudity prompts using the recommended hyperparameters for this task: a length of prompts (K) of 16 and a weight of empirical concept (η) of 3. For our evaluation, we generate one image for each of these 95 adversarial prompts, using the fixed seeds provided by RAB for reproducibility. The resulting images are subsequently evaluated using NudeNet to calculate the ASR.

- **CCE** [27]: This white-box attack employs Textual Inversion to optimize a new embedding vector (v_a^*) that serves as a proxy for the erased concept. For the Nudity task, to ensure a fair comparison with other baselines, we use the same 142 images from our UDA setup as the training set to optimize v_a^* on each sanitized model. For evaluation, we then prepend the learned v_a^* to the 142 corresponding prompts. For the Artistic Style (Van Gogh) task, we follow the original CCE protocol [27], using 6 images generated from “A painting in the style of Van Gogh” as the training set. We then evaluate by generating 50 images using the prompt “a painting in the style of v_a^* ”. For the Object (tench) task, we again adhere to the original CCE protocol, using 30 images of the object as the training set. Evaluation is then performed by generating 50 images using the prompt “A photo of v_a^* ”, aligning with the evaluation scale of other baselines. All inversion optimizations are trained for 1,000 steps with a learning rate of 0.005.

7. Ablation Study

To validate the necessity of our optimization procedure, we conduct an ablation study comparing our full TINA framework against two baselines (Figure 6): (1) a standard, text-guided DDIM inversion (Standard Inv.) and (2) a variant of TINA with insufficient optimization steps (TINA-Less). The results clearly demonstrate the importance of sufficient optimization. The text-guided Standard Inv. fails (30% ASR), as the erasure method actively counteracts the textual prompt. TINA-Less, which lacks sufficient optimization iterations to correct cumulative approximation errors, also performs poorly (46% ASR), producing distorted reconstructions. In contrast, our full TINA, which applies adequate optimization iterations to refine each inversion step, achieves high-fidelity reconstruction and a 70% ASR. This 24-point ASR improvement over TINA-Less demonstrates that a sufficient number of optimization steps is critical for accurately identifying latent generative trajectories, confirming the necessity of our

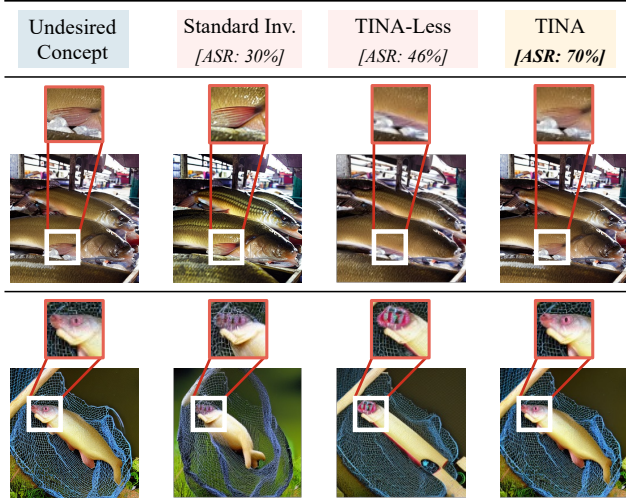


Figure 6. Ablation study of attack results on the ESD method for tench object erasure. From left to right: target concept, Standard Inv. (standard text-guided inversion), TINA-Less (with insufficient optimization), and our full TINA method.

iterative refinement procedure.

Figure 7 provides a complementary visual perspective on the role of optimization. When the text condition is directly set to null, the resulting inversion can still recover the coarse layout of the target image, but the reconstructed results often exhibit blurred local structures and weakened style-specific textures. This behavior indicates that the naive null-text DDIM inversion does not reliably trace a sufficiently precise generative trajectory for faithful concept recovery. By contrast, the optimization procedure in TINA yields reconstructions with sharper local patterns and more coherent stylistic cues, showing that its benefit lies not only in recovering the concept at a coarse semantic level, but also in preserving the fine-grained visual details that define the target concept.

8. Comparison with DDIM-Based Reconstruction Methods

To further contextualize the performance of TINA, we compare it against a recent state-of-the-art DDIM-based reconstruction method, EasyInv [58], which has been shown to outperform vanilla DDIM Inversion [37], Null-Text Inversion [23], Negative-Prompt Inversion [22], PnP Inversion [14], and others. To ensure a fair comparison, we configure EasyInv to operate under the same text-free condition as TINA. As shown in Table 5, our TINA significantly outperforms EasyInv across all five unlearning defenses on the tench object erasure task. This substantial performance gap demonstrates that general-purpose DDIM-based recon-



Figure 7. Visual comparison between naive null-text DDIM inversion and our optimized TINA inversion on the Van Gogh style erasure task. While the naive null-text DDIM inversion can roughly recover the global composition, it often fails to preserve fine-grained stylistic details, such as brushstroke textures and local structures. In contrast, TINA produces reconstructions with noticeably richer and more faithful visual details.

	EasyInv [58]	TINA
ESD [6]	24.0	70.0
EraseDiff [48]	26.0	68.0
SalUn [5]	30.0	72.0
Scissorhands [47]	34.0	78.0
STEREO [38]	24.0	72.0

Table 5. Attack Success Rates (ASR, in %) comparison between EasyInv and our TINA on the tench object erasure task. Both methods operate under a text-free condition. **Bold** indicates the best-performing method.

struction methods, even state-of-the-art ones, are insufficient for the concept recovery task, further validating the necessity of our tailored optimization-based inversion approach.

9. Generalization to DiT-Based Architectures

While the main experiments focus on UNet-based diffusion models (e.g., Stable Diffusion v1.4), an important ques-



Figure 8. Generalization of TINA to a DiT-based architecture (PixArt-XL-2-512x512). We erase the “Parachute” concept using ESD and then apply TINA. While the erased model fails to generate parachutes, TINA successfully recovers the concept, demonstrating architecture-agnostic generalizability.

tion is whether TINA generalizes to fundamentally different model architectures. To investigate this, we evaluate TINA on a Diffusion Transformer (DiT) [26]-based text-to-image model, specifically PixArt-XL-2-512x512 [3], which replaces the UNet backbone with a transformer architecture.

Since PixArt-XL-2-512x512 cannot generate the “Tench” concept used in our main experiments, we instead conduct this evaluation on the “Parachute” concept. Additionally, as there are no publicly available erased versions of this DiT model, we first apply the ESD [6] method to erase the parachute concept from the model, and then perform our TINA attack on the resulting erased model.

As shown in Figure 8, the erased DiT model is no longer able to generate the parachute concept under normal sampling conditions. However, our TINA method successfully recovers the erased concept, producing recognizable parachute images from the erased model. This result demonstrates that the vulnerability exposed by TINA is not limited to UNet-based architectures, but extends to DiT-based models as well, confirming the broad generalizability of our attack.

10. Failure Cases

While TINA consistently achieves the highest ASR across all evaluated defenses, its performance is not uniform. As reported in Table 2, TINA’s ASR against STEREO [38] on the artistic style erasure task is 44.0%, which, despite being the best among all evaluated attacks, is notably lower than its 70.0%–80.0% ASR against other defenses. This indicates that adversarially robust erasure methods can partially resist our text-free inversion attack.

To provide a concrete illustration, Figure 9 presents several failure cases drawn from the STEREO style erasure setting. In these examples, images reconstructed by TINA preserve the overall spatial structure and composition of the target, yet fail to recover the distinctive characteristics of Van Gogh style, such as the expressive brushwork, bold color palette, and textural impasto. We attribute this partial failure to two factors. First, the adversarial training procedure of



Figure 9. Failure cases of TINA on the STEREO style erasure (Van Gogh) task. While TINA preserves the spatial composition of the target images, the reconstructed results fail to recover the distinctive artistic style, indicating that the adversarial training procedure of STEREO partially disrupts the style-specific visual knowledge.

STEREO not only fortifies the text-image mapping against adversarial prompts but may also perturb the internal visual representations, making the stylistic knowledge harder to reactivate via a text-free trajectory. Second, unlike concrete objects or explicit content, artistic style is a high-level, distributed visual attribute whose encoding in the parameter space is inherently more diffuse and thus more susceptible to robust erasure. This also explains the discrepancy with the object erasure task, where TINA still achieves 72.0% ASR against the same STEREO defense (Table 4).

Nevertheless, these failure cases do not undermine our central thesis. Even in the most challenging setting, a 44.0% ASR of TINA demonstrates that a substantial portion of the visual knowledge persists within the erased model. Moreover, all text-centric baselines are entirely neutralized by STEREO on style erasure (0.0% for both P4D and UDA), whereas TINA still succeeds in a significant fraction of cases. These results suggest that while adversarially robust methods like STEREO represent a meaningful step forward, they still fall short of fully eliminating visual knowledge, reinforcing the need for erasure paradigms that operate directly on internal visual representations.

11. More Visual Results

We provide expanded qualitative comparisons in Figure 10 and Figure 11 to further demonstrate the fundamental vulnerability exposed by TINA.

Figure 10 presents a comprehensive matrix of attack results for the nudity erasure task. These visualizations visually substantiate our quantitative findings. A clear trend emerges for text-centric baselines (P4D, UDA, RAB, and CCE): while they show varying degrees of success against simpler defenses, their efficacy diminishes significantly against more advanced, adversarially-aware meth-

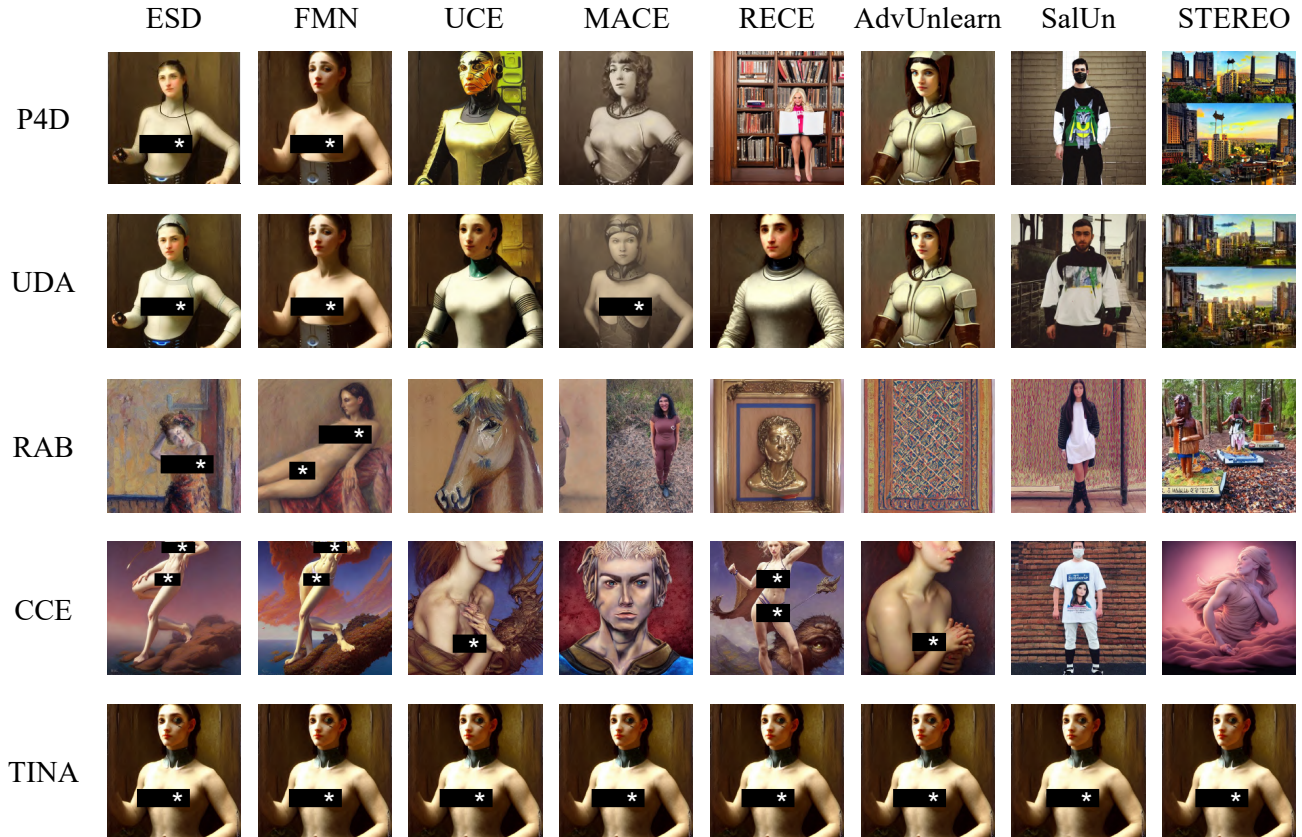


Figure 10. Qualitative comparison of attack methods on the nudity erasure task. Each row corresponds to an attack method, and each column corresponds to an unlearning defense. Sensitive content is redacted.

ods. Specifically, against robust defenses such as AdvUnlearn, SalUn, and STEREO, these attacks are almost entirely mitigated, producing neutral or unrelated imagery. In stark contrast, the bottom row shows that our TINA consistently bypasses all defenses, successfully uncovering the generative process to regenerate the forbidden content.

Figure 11 details the results for the Van Gogh style erasure. This figure not only reinforces the failure of text-based attacks (P4D, UDA) against robust defenses (AdvUnlearn, STEREO) but also reveals a critical flaw in embedding-space attacks. As shown in the third row, the CCE attack conflates the concept of “Van Gogh’s style” with “Van Gogh’s likeness.” Consequently, it predominantly generates portraits of Van Gogh himself, rather than applying the distinct artistic style to a general concept. TINA, however, does not suffer from this ambiguity. Operating independently of the text-conditioning path, TINA (bottom row) successfully isolates and reactivates the underlying generative trajectory for the style itself, proving that this visual knowledge persists even after robust erasure.

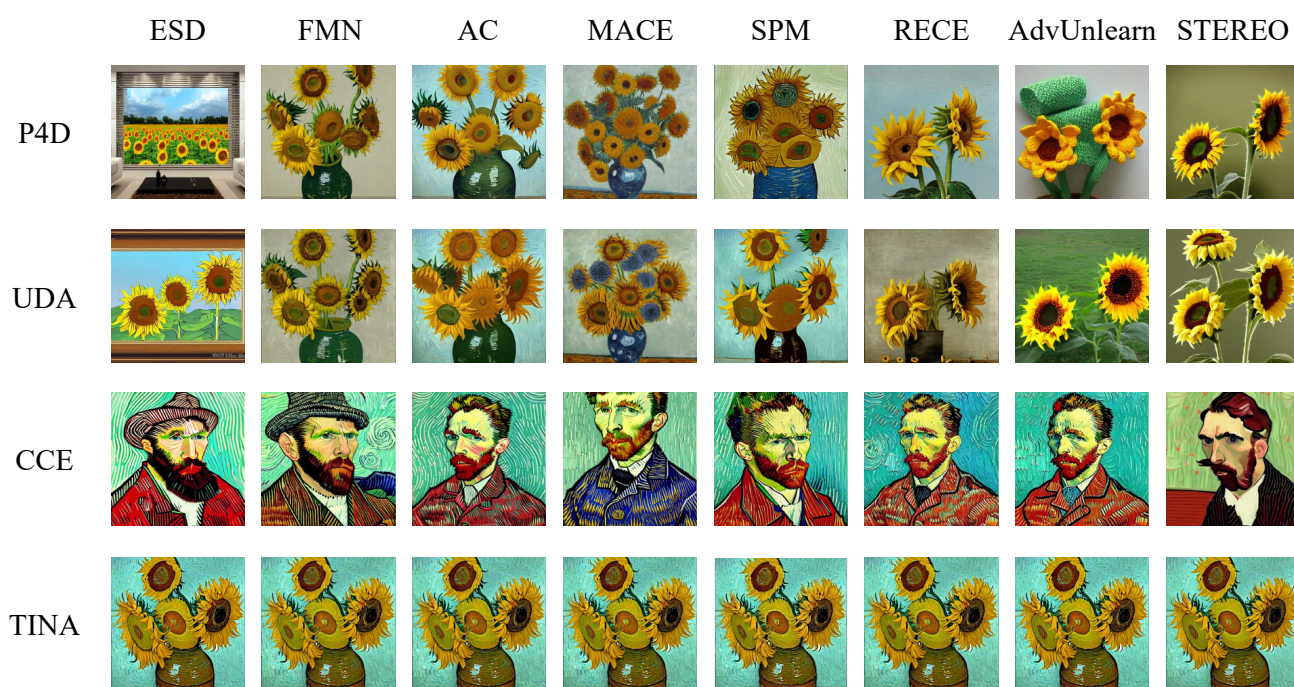


Figure 11. Qualitative comparison of attack methods on the “Van Gogh” style erasure task. Each row represents an attack, and each column represents a specific unlearning defense.